Desalination 397 (2016) 174–184

Contents lists available at ScienceDirect

Desalination

journal homepage: www.elsevier.com/locate/desal

An operational and economic study of a reverse osmosis desalination system for potable water and land irrigation

M. Sarai Atab [a,b], A.J. Smallbone [a,*], A.P. Roskilly [a]

[a] Sir Joseph Swan Centre for Energy Research, Newcastle University, Newcastle-Upon-Tyne, UK
[b] The University of Wasit, Wasit, Iraq

HIGHLIGHTS

- A reverse osmosis (RO) desalination plant for the MOD river in Iraq is presented.
- Variation of temperature, pressure and recovery in membrane module are considered.
- Water for drinking and irrigation applications are discussed.
- Salt rejection rates sensitivities to temperature and pressure are highlighted.
- An economic analysis is carried out to determine the total water cost (TWC).

ARTICLE INFO

Article history:
Received 17 March 2016
Received in revised form 7 June 2016
Accepted 19 June 2016
Available online xxxx

Keywords:
Reverse osmosis
Desalination
Brackish
Energy recovery
Potable
Irrigation

ABSTRACT

Desalination is a method for producing water for human consumption, irrigation or industrial utilisation. In this study, a reverse osmosis (RO) system for brackish water desalination was theoretically investigated to produce both potable drinking and agricultural water with a lower overall and specific energy consumption. As a case study, the Main Outfall Drain in Iraq is used as the brackish water source. A numerical model based on solution-diffusion theory was developed in Matlab Simulink and used to analyse the design and performance of an RO system. The effect of feed water temperature, pressure, salinity and recovery ratio on the efficiency of the whole RO system was investigated for a wide range of design considerations. The design of an RO system for this application was optimised and economic assessment carried out. Results show that with boosting recovery ratio from 30% to 60%, the specific energy of desalinated water production below 400 ppm was reduced from 2.8 kWh/m^3 to a more economically favourable value of 0.8 kWh/m^3, when utilizing a pressure exchanger as a recovery device. Salt rejection was reduced from 97% to 88% to obtain large quantities of water for irrigation with an acceptable salinity (<1600 ppm), for agricultural use. The reduction in salt rejection is influenced by the feed water temperature and pressure; also the average pore diameter of the RO membrane and in turn determines the reduction in system energy consumption. It was found that the total cost to produce 24,000 m^3/d of water from a feed salinity of 15,000 ppm and a water quality of <400 ppm would be 0.11 £/m^3 with a corresponding investment cost of £14.4 million for the drinking water, and for irrigation) obtained product <1600 ppm) are £0.9/m^3 and £11.3 million.

1. Introduction

In recent years there has been considerable growth in the utilisation of reverse osmosis (RO) processes in major desalination plants [1,2]. An RO purification system uses a semi-permeable membrane to remove ions, proteins, and organic chemicals which are generally not easily removed using other conventional treatments [3]. Among the benefits of RO are its small footprint, a modular design and the possibility of automatic process control and relatively low-cost of water production [4]. RO has been used widely for various water and wastewater treatment processes [5,6], in areas with scarce water supplies (as a means of seawater desalination) and importantly for this study the treatment of brackish water. However RO desalination suffers from a high energy input demand, fouling of the membranes, and low-quality of the water compared to thermal technologies which produce very high quality [2,3]. A high hydraulic pressure is required to overcome the osmotic pressure of the salinated feed water solution, which means a high consumption of energy is required when pressurizing the feed flow. Over the past 40 years, as a result of on-going technological advances [6] there has been a significant reduction in the energy required.

Abbreviations: BWIP, brackish intake and pre-treatment section; ERD, energy recovery device; HPP, high pressure pump; O&M, operating and maintenance; PEC, purchased equipment cost; RO, reverse osmosis; TCI, total capital investment.

* Corresponding author.
E-mail address: andrew.smallbone@newcastle.ac.uk (A.J. Smallbone).

http://dx.doi.org/10.1016/j.desal.2016.06.020

Nomenclature

A	Area, m^2
A_w	Permeability coefficient, m/s-Pa
B_s	Solute transport parameter, m/s
$\overline{C}$	Average salinity through the membrane element, mol/m^3
C_{ch}	Cost of chemical treatment, £/m^3
CD_m	Membrane cost, £
C_e	Unit power cost, £/kWh
C_f	Concentration of feed water, mol/m^3
C_m	Solute concentration in the membrane, mol/m^3
C_{RO}	Mass fraction of salt in permeate, %
C_p	Solute concentration at permeate, mol/m^3
C_r	Concentration in the concentrate, mol/m^3
C_w	Water concentration in the membrane, mol/m^3
D_w	Water diffusivity, m^2/s
D_s	Diffusivity of solute, m/s
E	Specific energy consumption, kWh/m^3
E_{ERD}	Turbine energy, kWh
Em	Membrane activation energy, J/mol
E_{pump}	Pump energy consumption, kWh
F_1	Plant load factor, %
GBP	Great British Pound, £
i_{eff}	Effective discount rate relation between the future value and present value
J_s	Solute transport, m/s
J_W	Permeate flux, m/s
K_s	Solubility of solute, m^2/s
N	Number of membrane elements
PC_m	Cost per membrane, £
P_f	Feed water pressure, Pa
P_{IP}	Pressure after the intake pump, bar
P_m	Annual membrane replacement factor, %
P_p	Permeate pressure, Pa
P_r	Rejected pressure, Pa
ΔP	Transmembrane pressure difference, Pa
Q_f	Feed flow rate, m^3/day
$\dot{Q}_f$	Daily feed flow rate after extracting the bypass ratio, m^3/day
Q_p	Permeate flow rate, m^3/day
$\dot{Q}_{p,a}$	Annual volume flow rate of product water, m^3
$Q_{p,\,el}$	Permeate flow rate per membrane element, m^3/s
$\dot{Q}_p$	Mass flow rate of permeate in one element, kg/s
Q_r	Rejected flow rate, m^3/day
Q_{bypass}	Amount of water mixes with the permeate to achieve the required salinity, m^3
R	Gas constant, J/mol-k
r_n	Nominal escalation rate which effects of resource depletion, increased demand and inflation, %
r_r	Recovery ratio, %
R_s	Salt rejection, %
T	Temperature, K
TCF	Temperature correction factor at T, %
V_w	Water molar volume, m^3
$\dot{W}$	Work, kW

Greek symbols

δm	Membrane thickness, m
η	Efficiency, %
$\Delta\pi$	Osmotic pressure difference, Pa

Subscripts

E	Energy
f	feed water
IP	Intake Pump
m	membrane
p	permeate
r	rejected

Nevertheless, the overall energy utilisation remains considerable for RO desalination and as such the cost-effectiveness of production is highly sensitive to changes in energy prices and policy decisions related to greenhouse gas emissions. Typically, in an RO plant, the production of one cubic meter of freshwater from seawater uses 3–10 kWh of electricity, and between 0.5 and 2.5 kWh from brackish water [7–9]. Another challenge with RO systems is the disposal of brine – an output which has a potentially damaging impact on the local marine environment. The accumulation of solids in the feed solution on the surface of the membranes, *i.e.* membrane fouling, is a further challenge for an RO system [10]. In fact, this is particularly significant where RO is employed for the wastewater treatment especially where the feed water contains a large amount of solids. Membrane solids is a complex phenomenon involving the deposition of several types of solids on the membrane surface. If it occurs, the permeability of the RO membrane is lowered, which in turn affects the energy requirement [11]. Suitable pre-treatment technologies can minimise membrane fouling to some degree, although it will also have its own energy demands. Improved rejection can be achieved by adding treatment stages or polishing steps, which would lead to substantially higher capital and running costs.

Much work has been carried out to reduce these limitations of RO desalination, including the development of novel membranes with high permeability to water but low permeability to salt [11]. In order to reduce energy consumption and fouling, investigations have been carried out into the hydrodynamics of feed flow inside an RO membrane module. Consideration has been given to various techniques for pre-treatment and post-treatment in combination with the analysis of the characteristics of the feed water. The success of an RO system design requires robust analysis at the feasibility stage to evaluate alternative designs for more efficient design and operation, which can be later applied in its construction. Although membrane manufacturers have developed numerical models to support the design process, the principal area of attention has been on their performance rather than the optimisation of the complete desalination in terms of energy consumption and product water quality. Some research [12–14] has investigated the development of new models for the optimisation of membrane modules and the desalination plant. Nevertheless, the focus of previous research has not been on the impact of various designs and operating conditions on RO desalination performance [15–21]. In addition, several cost models have been developed during recent years; however, they were mostly focused on domestic and municipal [22,23]. Nonetheless, economic data of brackish water on industrials for drinking and irrigation in literature are significantly limited [24–26]. Any system analysis should be underpinned by a feasibility study which supports the selection of appropriate technologies for characterisation of the capital operating and investment costs. The main aims of this paper are to construct a numerical model of an RO system, with and without energy recovery, validate the model against reported measurement data, study the effect of operating parameters such as temperature, salinity, pressure and recovery ratio on RO efficiency, and optimize the RO desalination system in terms of energy requirement, salt rejection and total cost of water production.

2. Case study

Iraq has been experiencing an extreme water shortage in recent years, over the last four decades the amount of available water has diminished because of the use by upstream countries such as Turkey and Syria [27]. Recently, agricultural lands have been adversely affected by these shortages, and there is a need for a very large quantity of water

Fig. 1. Map shows the Euphrates, Tigris and MOD river and the main Mesopotamian marshlands.

Table 1
Chemical properties for several places on the MOD.

Zones		M1	M2	M3	M4	M5	M6	M7	M8	M9	M10
PH		7.68	7.28	6.99	7.52	7.05	7.54	6.92	7.12	7.24	7.90
Electrical conductivity (ds/m)		2.92	3.8	5.10	7.31	7.76	9.55	9.52	10.53	14.02	14.96
TDS (mg/l)		1868	2432	3264	4691	4966	6112	6092	6739	8972	9574
Dissolved positive ions (mg/l)	Ca	1050	1000	1500	1215	1466	300	2975	720	670	8800
	Mg	350	385	550	330	520	170	987	390	180	2960
	K	14	14.5	14.5	14	15	8.0	18.5	18.5	10.5	8.0
	NH_4	0.65	8.89	9.38	4.93	0.26	0.29	0.86	6.16	0.76	7.67
Dissolved negative ions (mg/l)	NO_2	0.012	0.028	0.044	0.007	0.010	0.055	0.017	0.009	0.017	0.006
	SO_4	1585	1823	2272	1842	2089	913	3230	1141	1031	4955
Cl (mg/l)		1738	1624	2669	1897	2692	568	5680	1363	874	1848
Alkalinity (Mg/l)		175	220	290	235	250	160	135	195	165	150
Total organic carbon sediment (TOCS) (%)		0.12	3.12	2.23	3.5	0.38	0.28	0.23	1.44	1.53	1.34

to revive the dried marshlands in Southern Iraq. The Mesopotamian marshlands are the largest wetlands ecosystem in the Middle East and western Eurasia. They are crucial in terms of ecological, economical and hermetic importance, but they are in drought [28–30]. The special significance of these marshlands are habitat provided for migratory birds support for endangered species and the support provided for

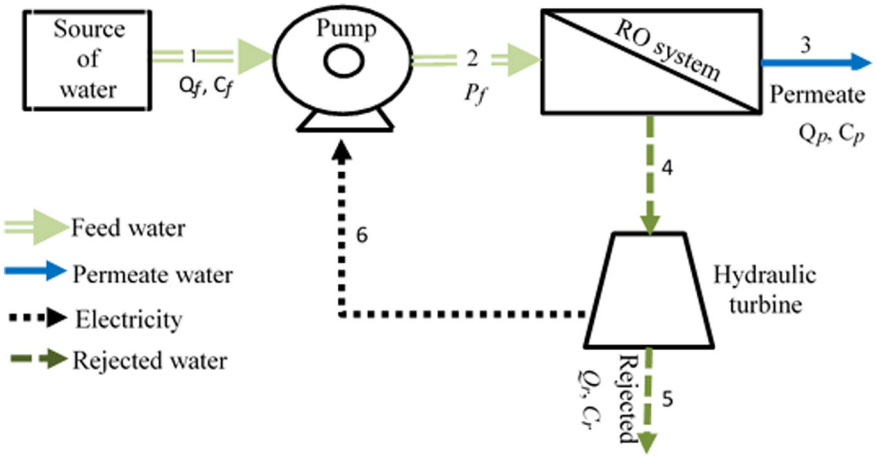

Fig. 2. Schematic representation of the RO desalination model with turbine energy recovery system.

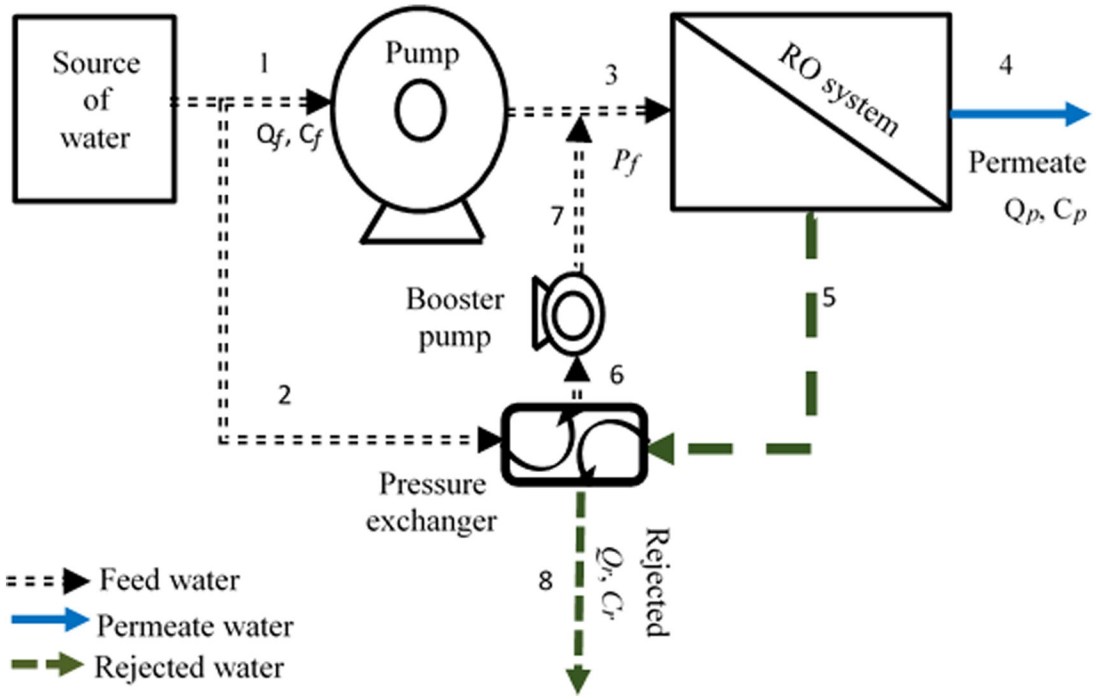

Fig. 3. Schematic representation of the RO desalination model with PX energy recovery system.

freshwater fisheries. Aboriginal communities have been living in these marshlands for millennia and include culturally significant historical sites such as the Garden of Eden [28–30].

Around 150,000 km^2 of Iraqi agricultural lands drain into by the Main Outfall Drain [1], formerly called The Third River, shown in Fig. 1. The MOD is situated between the Tigris and Euphrates Rivers, and passes through the main Mesopotamian marshlands south of these rivers. This work considers that the MOD river could provide Southern Iraq with a lifeline for potable and irrigation water and could supply water for 1.8 million people in All-Nasiriya City and irrigate 150,000 km^2 of farmland and replenish 20,000 km^2 of the southern marshlands [31].

According to the Iraqi Ministry of Agriculture, the river has suffered from very high salt concentrations since it was constructed in 2008. It has a length of 565 km from north of Baghdad to the Arabian Gulf with the total discharge of 210 m^3/s. Drainage water is released into Shat AL Basra canal and then flows into the Arabian Gulf. The chemical properties of the water for different zones Fig. 1 close to Al-Nasiriya City are shown in Table 1 [32]. The salinity level increases gradually as it flows from the south of Iraq close to city of All-Nasiriya with total dissolved solid (TDS) levels between 6000 and 8500 ppm [33]. Recently, the MOD water has been used to revive the dried marshlands but this has resulted in a negative effect on diversity of life and agricultural due to its high salinity. Therefore, to satisfy the demands of agricultural irrigation, marshland revival and domestic water user the desalination of some of the MOD water would be hugely beneficial.

3. Model development, model based analysis and optimisation

The Matlab/Simulink and Thermlib blocks software tools were used to design an RO system numerical model. The schematic diagram of the RO desalination system with Turbine is shown in Fig. 2 and with Pressure exchanger is shown in Fig. 3, and the modelling equations as shown in Table 2. The main components of the RO system are a pump unit which supplies high pressure feed water, P_f and flow rate, Q_f to a membrane, a group of membrane modules, and an energy recovery device (hydraulic turbine and pressure exchanger) which generates energy from the rejected brine stream and directly powers a pump. The model was designed to predict the system performance and support

Table 2
Summary of RO model equations.

Meaning	Equation	No.	Reference
Permeate flux	$J_W = A_w(\Delta P - \Delta\pi)$	1	[36,38,40]
Solvent permeability coefficient	$A_W = \frac{D_w C_w V_w}{\delta_m RT}$	2	[36,40,41]
Solute transport	$J_s = B_s(C_m - C_p)$	3	[38–40,42]
Solute permeability coefficient	$B_s = \frac{D_s K_s}{\delta_m}$	4	[40,41]
Salt rejection	$R_s = [1 + \frac{B_s}{A_w(\Delta\rho - \Delta\pi)}]^{-1}$	5	[40]
Osmotic Pressure	$\Delta\pi = RT\sum(n/v)$	6	[38,41]
Temperature correction factor	$TCF = , exp[\frac{E_m}{R}(\frac{1}{273+T} - \frac{1}{298})]$	7	[43,44]
Specific energy	$E = \frac{P_f Q_f (E_{pump})^{-1} - P_r Q_r E_{ERD}}{Q_p}$	8	–
Recovery ratio	$R = \frac{Q_p}{Q_f}$	9	–
Total mass balance	$Q_f C_f = Q_p C_p + Q_r C_r$	10	–
Delta pressure	$\Delta P = \frac{P_f + P_r}{2} - P_p$	11	–

Table 3
Model validation for RO model against reported measurement data.

Parameters		Unites	Reported measurement data	Model	Percentage error
Normal flow	Feed	T/H	327.6	327.58	0.01%
	Permeate	T/H	147.4	147.41	0.01%
	Rejected	T/H	180.2	180.17	0.6%
Temperature	Feed	°C	25–34	25	–
	Permeate	°C	25–34	25	–
	Rejected	°C	25–34	25	–
Pressure	Feed	bar	64	65	1.5%
	Permeate	bar	1.5	1.5	–
	Rejected	bar	62	63	1.5%
Total Dissolved Solids (TDS)	Feed	mg/l	36,000	36,036	0.1%
	Permeate	mg/l	500	477	4.8%
	Rejected	mg/l	65,100	65,130	0.05%

Table 4
The RO modelling conditions.

Temperature, °C	TDS, kg/kg	Pressure, bar	Q_f, m^3/h	C_p, ppm
25	0.015	30	2224	<400

the optimisation of the permeate quality and flow rate. In this paper, the following assumptions were imposed:

- the solution-diffusion model is valid for the transport of water and solute through the RO membrane;
- the efficiency of the pump and turbine are fixed at 84% and 70% respectively;
- The pressure drop in feed stream is taken as the dead state 101.3 kPa;
- the salt feed water stream is considered to be a dilute solution and is treated as an ideal solution;
- the concentration polarization effect is negligible; [21,34,35].

The solution-diffusion model formed the basis for the design of the model. The difference between permeability coefficient, A_w and solute transport parameter, B_s determines the separation performance of the RO system. Any excess of the hydraulic pressure applied, P_f was assumed to be proportional to water permeation over the osmotic pressure, π_m. Where J_W is the permeate flux, A_w is the apparent water permeability of the membrane which is used to characterise the membrane itself, ΔP is the pressure applied across the membrane, and $\Delta\pi$ is the osmotic pressure difference between the feed and the permeate [36,37]. Furthermore, the flux of the dissolved salts is proportional to the *trans*-membrane concentration difference. However, A_w and B_s, are dependent upon temperature and they can be defined by a viscosity temperature function which is considered to have sufficient accuracy for engineering analysis carried out here. Changes in A_w result in proportional changes in J_w and J_s, which means the temperature dependency of A_w and B_s must at least in principle be considered. For practical purposes, however, the temperature dependency of B_s is often neglected, while only the temperature dependency A_w, which is much more important is included. The selectivity of a membrane considered, using the rejection coefficient, which explains the more frequent use of a rejection coefficient R and permeate flux J than the use of A_w and B_s membrane constants. However, such use of R and J only has significance when linked with precise information regarding the conditions, *i.e.* transmembrane pressure difference, salt concentration of the feed solution and membrane flux conditions. Thus, the formation of a concentration layer occurs at the membrane surface: The strong effect of concentration is hidden in the osmotic pressure difference $\Delta\pi$. At least for highly dilute solutions, the relationship between osmotic pressure and concentration is linear: The transmembrane osmotic pressure is determined by Eq. (1). Membrane salt rejection is a measure of performance for overall membrane system for example manufacturers of membrane technologies usually define a specific salt rejection for each

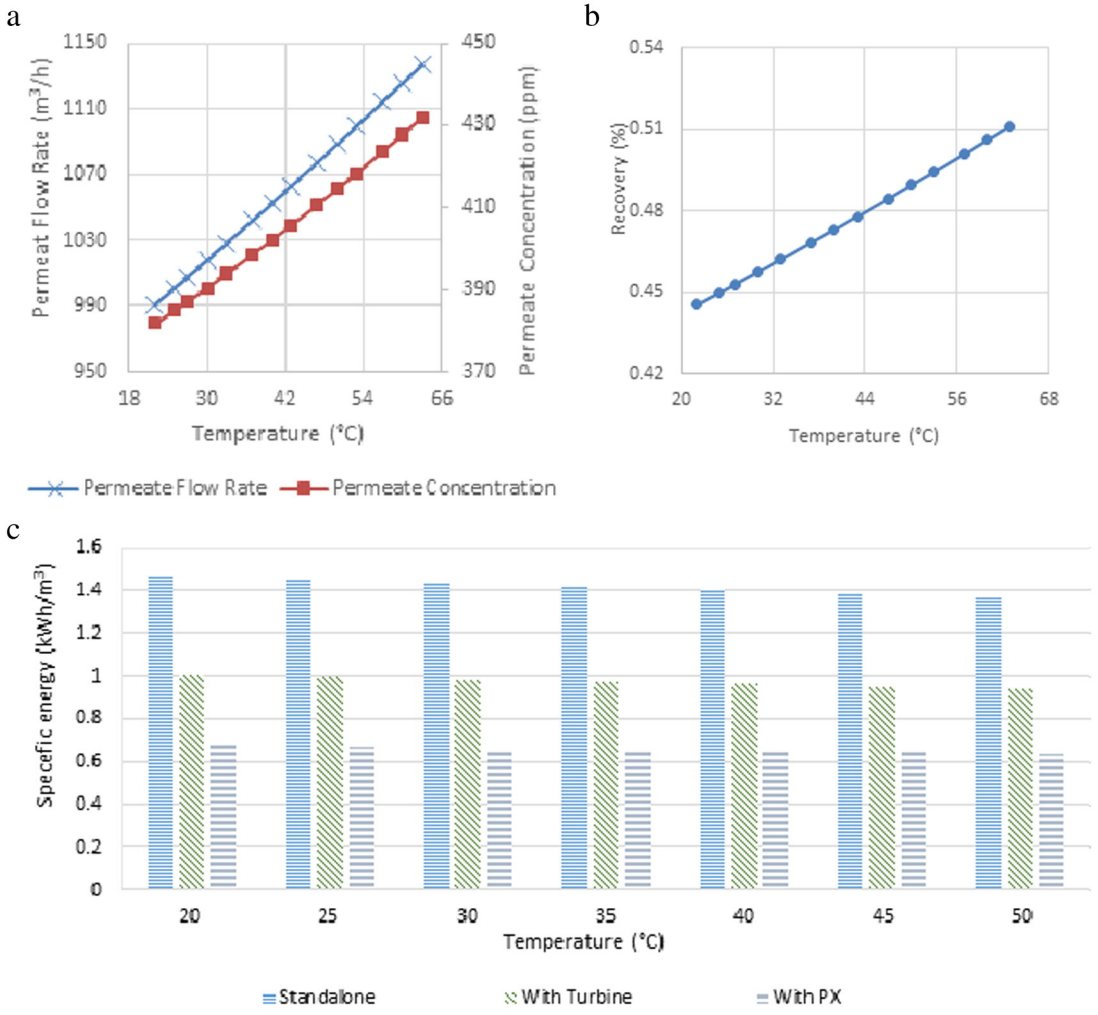

Fig. 4. Utilizing operating parameters as function of temperature.

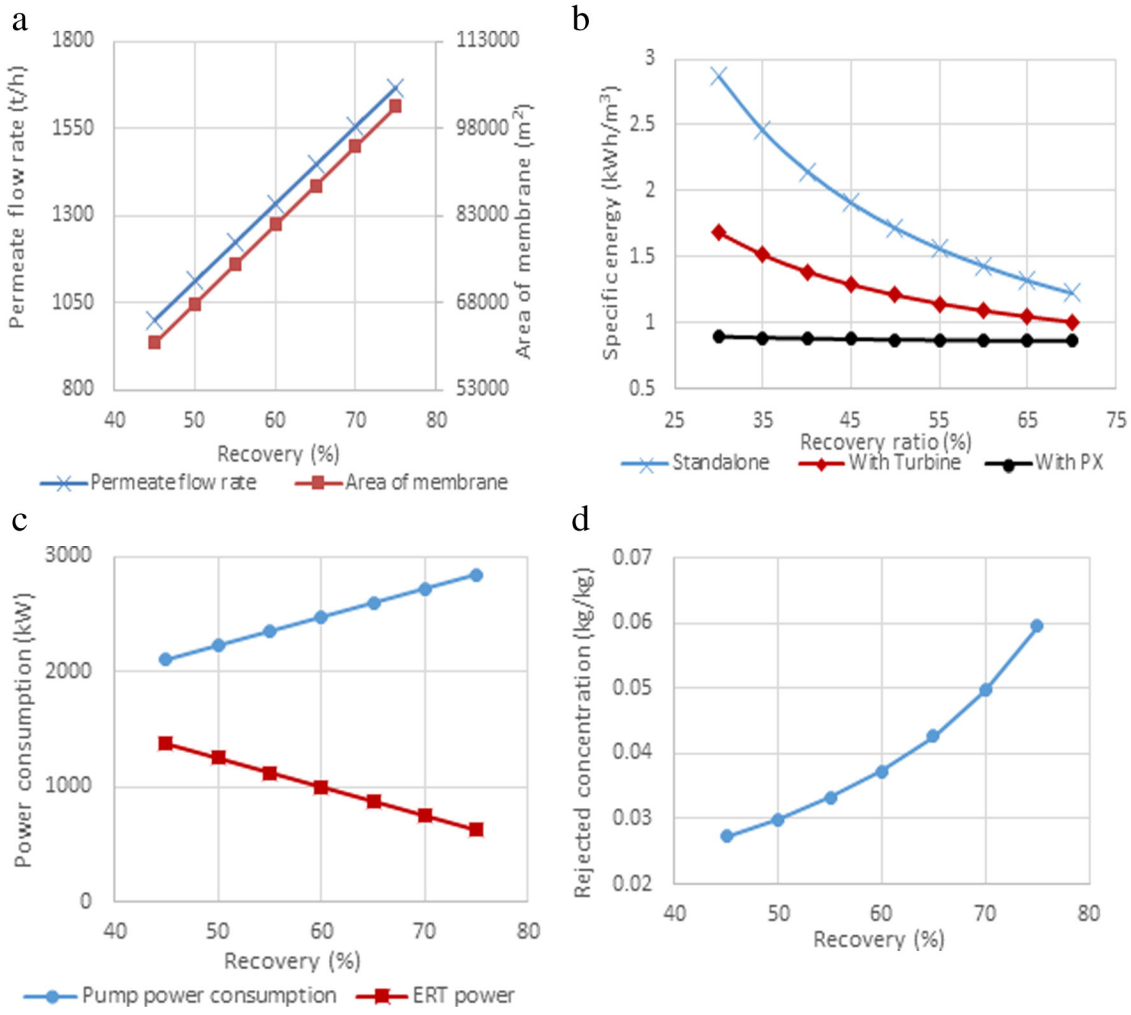

Fig. 5. Effect of Recovery on permeate flow rate, area, power consumption and specific energy.

commercial membrane available. Salt rejection through an RO membrane is nominally given by:

$$R_s = \left(1 - \frac{C_p}{C_r}\right) * 100\% \tag{12}$$

The feed water becomes gradually concentrated from the beginning to the end of the tube in a spiral wound element, and the salt rejection is described by:

$$R_s = \left(1 - \frac{C_p}{\left(\frac{C_f + C_r}{2}\right)}\right) * 100\% \tag{13}$$

Where C_r is the ion concentration in the concentrate. RO membranes achieve NaCl rejections of 98–99.8% [45].

The stream numbers on the schematic representation are indicators of thermodynamic properties, as shown in Figs. 2 and 3. Stream no.1 is used as feed water which takes on the properties of brackish water for the purposes of validation. The RO model was built and validated against previously reported measurement data [46]. Table 3 establishes the difference between the RO model and reported measurement data as <4.8%.

4. Results and discussion

4.1. Effect of feed water temperature and recovery on RO efficiency

Based on the model conditions outlined in Table 4 and as a result of temperature increase mechanisms, the water passes more easily through the membrane due to a reduction in the water viscosity and change in the structure of membrane. As presented in Fig. 4(a), both the permeate flow rate and concentration increase with temperature from 20 °C to above 50 °C and this leads to increase of recovery, results in an increase in the mechanical power consumption (Fig. 4(b)). These outcomes are in good agreement with other reported observations [47,48,49] of similar systems. Furthermore, temperature plays a significant role in the performance of the RO filtration. For these calculations, the temperature range applied was between 20 °C and 50 °C. The specific energy increases with reducing temperature because of the corresponding reduction of the solvent transport constant, A_w (Eq. (2)), and the reduction of permeate flow rate (Eq. (7)). Fig. 4(c) shows the specific energy consumption for different scenarios, by using the pressure exchanger, the specific energy is reduced by about over 50% and by using turbine is about 30%. However, the concentration of TDS in the permeate decreased with the reduction in temperature, leading to a more considerable rejection of TDS. It should

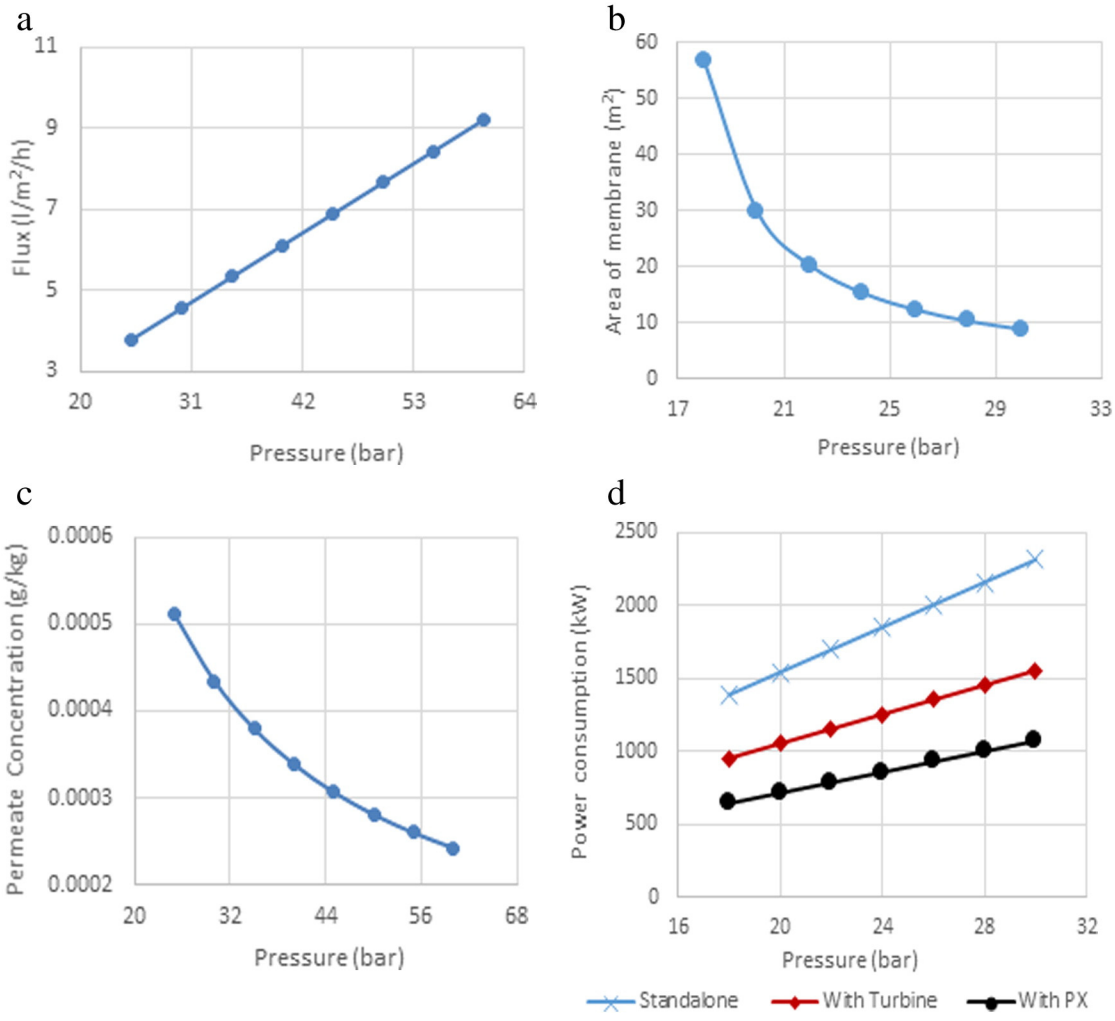

Fig. 6. Effect of pressure on permeate concentration, flux, area, ERT and PX power saving.

be noted that both the solvent transport constant, A_w in Eq. (2) and the solute transport constant, B_s in Eq. (4) increase with increases in temperature. By rearranging Eqs. (1) and (3), the solute concentration in permeate can be expressed as:

$$C_p = \frac{C_m}{\frac{A_w}{B_s}(\Delta p - \Delta \pi) + 1} \tag{14}$$

Hence, there is trade-off between temperature dependence of A_w and that of B_s which ultimately determines the overall temperature dependence of solute rejection. In addition as shown in Fig. 4(b), the percentage of recovery is effected by temperature which increased from <45% to >50% at 20 °C and 60 °C respectively.

Furthermore, the specific energy and membrane performance are influenced by the percentage of recovery. As shown in Fig. 5(a), with an increases in recovery percentage, the driving force required for an increase in flux increases due to greater salt concentration in feed stream, so the corresponding permeate flow rate increases thus requiring a large area of membrane. Production of high quantity of permeate water is positively affected on the specific energy which is reduced from 2.8 kWh/m^3 to a more economical 0.8 kWh/m^3 at 30% and 60% respectively, when using pressure exchanger, as shown in Fig. 5(b). Due to relatively high energy demands, most RO systems are fitted with a device to recover energy from the pressurized RO concentrate leaving the system. The primary objective here is to recover as much of the energy held in the pressurized RO concentrate stream as possible, and it is very clear from Fig. 5(b), the PX device is the best option to recover the rejected energy. The concentrate is sent through an energy recovery device, and this energy is used to supplement the power to the pumps. Thus the efficiency of the energy recovery device has important role in the overall RO system energy consumption. Fig. 5(c) demonstrates a high level of pump power consumed without any energy recovery compare with ERT consumption. In circumstances where the brine flow rate,

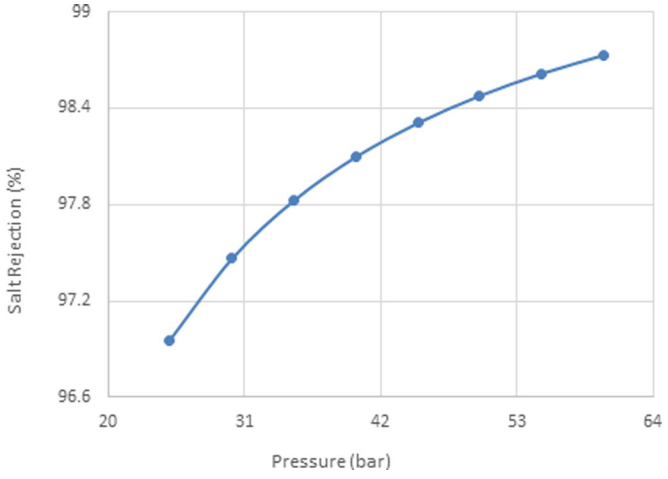

Fig. 7. Dependence of salt rejection on pressure.

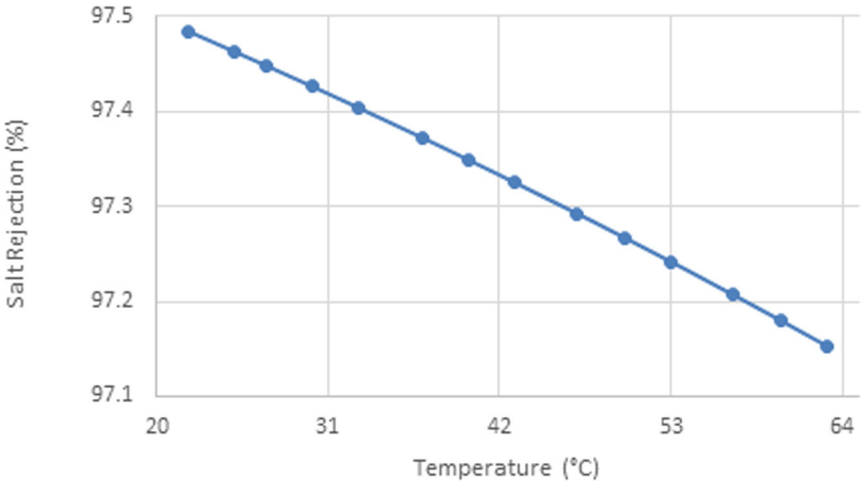

Fig. 8. Salt rejection as a function of temperature.

Q_r is low, and at a high recovery ratio, the efficiency of the energy recovery device has a diminished significance, as shown in Fig. 5(c), and increased the concentration in rejected (Fig. 5(d)).

4.2. Effect of applied pressure on permeate concentration, area of membrane, ERT power saving and flux

The performance of RO membrane was analysed at different feed water pressures. Fig. 6(a) shows the changes in permeate flux at different applied pressure with constant temperature (25 °C). In general, the results illustrated that an increase in applied pressure yielded in an increase in the feed water flux. These data are in agreement with the observations of Ahmed et al. [50], Mohammadi et al. [51] and Hyun et al. [48]. Based on Darcy's law, the permeate flux increases with increasing pressure gradient (see Eq. (1)) whereas, the membrane area decreases, as shown in Fig. 6(b). The solute concentration decreased gradually as the feed pressure increased, indicating that less permeate TDS is produced. Fig. 6(c) illustrates the concentration of permeate is reduced with increasing pressure. As shown in Fig. 6(d), another interesting observation was that the energy recovery turbine saved energy by approximately 30% by increasing the applied pressure and PX device saved >50%.

4.3. Salt rejection as function of temperature and pressure

Salt rejection coefficient is an appropriate measure for the selectivity of a membrane and is more often used than the membrane constants A_w and B_s (shown in Eqs. (2) and (4)) [52]. Whilst, the rejection coefficient is not a membrane constant, it is a function of the operating conditions. Fig. 7 shows that high pressures increase the salt rejection from 96.8% to >98.8% when pressure is increased from 25 bar to 63 bar (at 25 °C). Also, salt rejection increases with reducing temperature as shown in Fig. 8, which means that with higher temperatures, much more TDS is in permeate. This is due to a reduction of solvent viscosity and the pore size

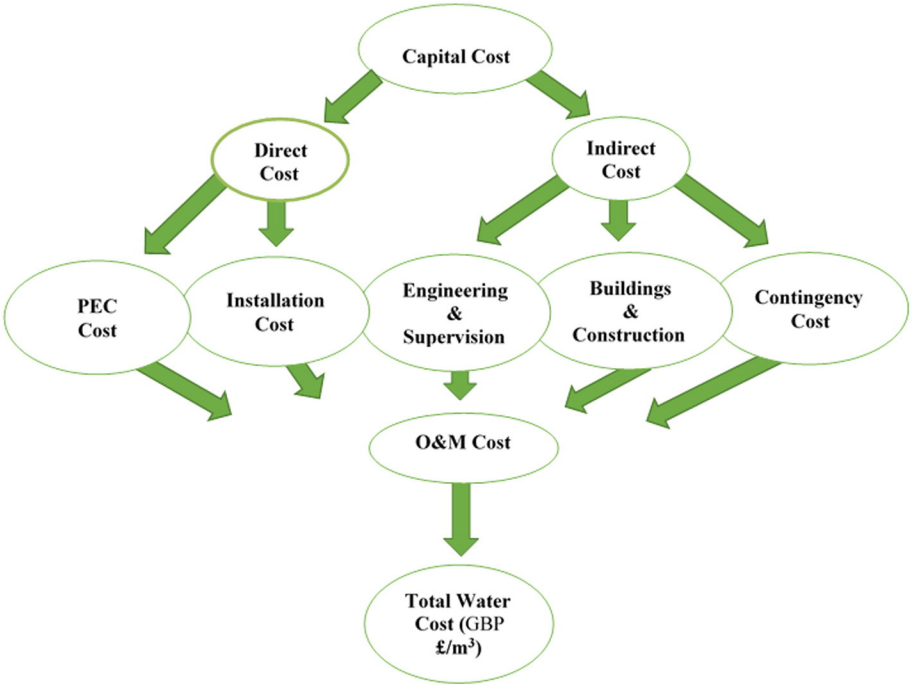

Fig. 9. Diagram of total water cost components.

Table 5
Economic data of the BWRO plant.

Economic parameters (assumed)	
Interest rate	8%
Nominal escalation rate, r_n	5%
Economic life time, n	16 year
Effective discount rate, i_{eff}	8%
Membrane life	5 year
Annual operating hours	7884 h

Table 7
Capital and operating costs.

Cost of chemical treatment, GBP £/m^3	0.00007
Cost of cartridge filters replacement, GBP £/m^3	0.004
Fixed cost, GBP £/m^3	0.015
Variable cost, GBP £/m^3	0.018
Cost, GBP £/kW	0.08
Total investment cost, GBP £ million	19.3
TWC, GBP £/m^3	0.11

effect. Both temperature and pressure regulate the amount of TDS in permeate. In order to produce higher quantities of water with specific quality (*i.e.* for irrigation applications), particularly with brackish feed water, control of the salt rejection ratio has been analysed. When salt rejection coefficient increases, less salt concentration appears in permeate and simultaneously higher energy is required. Thus, to mitigate the excess salt rejection, the pore size diameter can be increased. To match the feed brackish water in the proposed case study, with its specific requirements of freshwater properties and energy consumption, a change in salt rejection coefficient offers a viable solution. While, an increase of temperature affected the permeate concentration and flow rate, it proved insufficient to meet the requirements of freshwater production volume. Therefore, physical changes of pore size diameter for RO membrane are required to tackle the agricultural demand for water.

5. Economic analysis

Among the major determining factors for estimating the cost of water is the cost of available energy. The principal cost factors considered include capital investment, maintenance cost and the cost of supplying saline water to the desalination system. The labour cost can vary greatly, and is subject to the local economy. Cost balance equations for the required components in the system are presented in Table 6. The expenditure connected with setting up and operation of a desalination plant, include the initial concept, design, obtaining of permits, finance, construction and the commissioning and acceptance testing for normal operation [53] is defined here as the capital cost [24].

The total water cost (TWC) is estimated by adding the capital cost to the operating cost for the length of the contract (Fig. 9) and dividing the total of the amortized (annualized) capital costs and the annual Operating and Maintenance (O&M) costs by the average annual potable water production volume. These parameters are set out Tables 5 and 8. As is typical, the TWC excludes distribution costs, especially where alternative delivery contracts are concerned [53]. The O&M costs are specific to the site but consist of both fixed (insurance and amortization) and variable costs (cost of labour, energy, consumables, maintenance, and spare parts *etc.*). Features of capital cost are direct (process equipment, auxiliary equipment and the associated piping and instrumentation, site civil works, intake and brine discharge infrastructures, buildings, roads and laboratories) and indirect costs. The contract agreement establishes the land cost, which may vary from zero to an agreed lump sum according to the site characteristics [54]. Typically, 50–85% of the total capital cost are construction costs. Indirect capital costs, usually calculated as a percentage of the direct capital costs, averaging 40% [54], 15–50% [53] or 30–45% [55], but very project specific, are composed of interest accruing during construction, working capital, freight and insurance, contingencies, import duties, project management, and Architectural and Engineering (A&E) fees.

The TWC and the investment costs for the MOD brackish water plant are GBP £0.11/m^3 and GBP £14.4 million respectively. This is to produce drinking water with total capacity of 24,000 m^3/day (obtained product <400 ppm) and feed salinity of 15,000 ppm with PX device. Also the TWC and the investment costs production for irrigation) 24,000 m^3/day, feed salinity of 15,000 ppm and obtained product <1600 ppm) are GBP £0.9 /m^3 and GBP £11.3 million respectively. As shown in Fig. 10, the cost of production is affected by recovery devices, pressure exchanger reduced the cost by 11% of the cubic meter of the production and the turbine is only 3%, and these costs are influenced by the different salinities. These costs are in good agreement with the findings outlined in Tables 9 and 10. Comparing the model results of this work with findings of previous publications (Tables 9 and 10) confirms the rapid decline in TWC with increasing plant capacity. It can be concluded that the MOD investment cost and TWC arrived at in this work is in agreement with other findings. The annual investment cost

Table 6
Equations of calculation of the capital and operating cost.

Description	Equation	No.	Ref.
Cost of the intake and pretreatment	$\dot{C}_{BWIP} = 996.(Q_f)^{0.8}$	15	[26,56]
Annual cost of the energy of the intake pump	$\dot{C}_{e,BWIP} = \frac{P_{IP}.Q_f}{\eta_{IP}}.C_e.f_1$	16	[57,58]
Cost of chemical treatment in the pretreatment	$\dot{C}_{e,op,ch} = Q_f.f_1.C_{ch}$	17	[58,59]
Power of high pressure pump	$log_{10}(PC_{HPP}) = 3.3892 + 0.0536\,log_{10}(\dot{W}_{HPP}) + 0.1538[log_{10}(\dot{W}_{HPP})]^2$	18	[60]
Annual cost of the power provided to the HPP	$\dot{C}_{e,HPP} = P_{HPP}.\dot{Q}_f.f_1.C_e/\eta_{HPP}$	19	[58]
Capital cost of the RO membrane	$PC_{RO} = N\ .PC_m$	20	[26,57]
No. of elements	$N = r_r\ .\ \dot{Q}_f/Q_{p,el}$	21	[26,57]
Cost per membrane	$PC_m = 10.A$	22	[26,58]
Area	$A = \dot{Q}_p.\frac{C_{RO}}{B_s(\overline{C}-C_{RO})}$	23	[26,61]
Average salinity through the membrane element	$\overline{C} = \frac{(Q_f-Q_{bypass})C_f+Q_r.C_r}{Q_f-Q_{bypass}+Q_r}$	24	[26,61]
Amount of bypass water	$Q_{bypass} = Q_p[\frac{C_p-C_{RO}}{C_f-C_{RO}}]$	25	[26,61]
Cost of membrane elements replacement	$\dot{C}_{RO} = N.P_mCD_m$	26	[26,62]
Power of turbine	$log_{10}(PC_T) = 2.2.476 + 1.4965\,log_{10}(\dot{W}_T) - 0.1618[log_{10}(\dot{W}_T)]^2$	27	[60]
Total annual O&M cost	$\dot{C}_{O\&M} = 0.082X\ f_1\ X\ \dot{Q}_{p,a}$	28	[63]
Constant escalation levelization factor	$CELF = CRF.\frac{K(1-K^n)}{1-K}$	29	[64]
Constant factor	$K = \frac{1+r_n}{1+i_{eFF}}$	30	[64]
Capital recovery factor	$CRF = i_{eFF}.\frac{(1+i_{eFF})^n}{(1+i_{eFF})^n-1}$	31	[64]

Table 8
BWRO plant operating and design parameters.

Product water flow rate	24,000 m^3/day
Salinity of product water	<400 ppm
Brackish water salinity	15,168 ppm
Brackish water feeding temperature	25 °C
High pressure pump efficiency	84%
Pelton turbine efficiency	80%
Pressure exchanger efficiency	98%
Plant load factor, F_1	90%
Membrane recovery ratio, r_r	45%
Membrane replacement factor, P_m	10%
Membrane salt rejection ratio, R_s	97%
Water permeability coefficient, A_w	4.47×10^{-5} m/[s ∗ bar]
Nacl permeability coefficient, B_s	1.2×10^{-4} kg/[m^2 ∗ s]
Dead state temperature	25 °C
Number of streams	6
Pump pressure	30 bar

Table 9
Capacity of desalination unit and cost of water produced.

No.	Type of feed water salinity, ppm	Plant capacity, m^3/d	Cost, GBP/m^3	Source of information
1.	Brackish, 5700	50	4.7	[65]
2.	Brackish	<20	3.3–7.5	[9]
3.	Brackish	20–1200	0.45–0.77	[9]
4.	Brackish, 8116	6000	0.22	[66]
5.	Brackish, 4221	10,000	0.15	[66]
6.	Brackish, 5844–11,688	30,000	0.18	[66]
7.	Brackish, 10,000	~38,000	0.35	[67]
8.	Sea water, 26,000	~95,000	0.34	[67]
9.	Brackish, 3000	~38,000	0.21	[67]
10.	Brackish, 2300	~92,000	0.19	[68]
11.	Brackish, 5000	46,000	0.17	[69]
12.	Brackish	5000–60,000	0.15–0.31	[70]
13.	Brackish	40,000–46,000	0.15–0.31	[9]
14.	Brackish	19,000	0.15	[9]
15.	Brackish	Large scale	0.13–0.26	[7]
16.	Brackish	38,000	0.12	[9]

Calculation is based on the assumption that

1 GBP = 1.54 $
1 GBP = 1.37 €.

Table 10
Water and capital cost for different projects [7,67].

Feed water TDS, ppm	Capacity, m^3/d	Capital cost, GBP million	Cost, GBP/m^3
Sea water	20,000	13	0.42
Brackish water, 1380	28,400	16	0.2
Sea water	34,000	40–60	0.25–0.41
Sea water	45,000	45.5	0.36
Brackish water, 2550	55,670	56.5	0.27

Calculation is based on the assumption that

1 GBP = 1.54 $
1 GBP = 1.37 €.

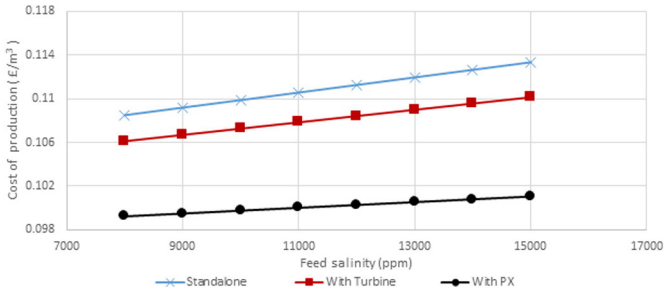

Fig. 10. Cost of production for different scenarios.

of any component is achieved by adding the annual total capital investment rate and the annual O&M cost rate, estimated by dividing the capital investment cost for each component by the plant annual operating hours, as shown in Tables 5, 7 and 8.

6. Conclusion

Numerical analysis has been conducted to study the performance of reverse osmosis membrane for a brackish water desalination process. The RO model has been designed for analysis of a case study based in Iraq and the model developed using Matlab/Simulink and Thermolib software. The process can produce water for several purposes namely for domestic utilisation, agricultural irrigation and survive Marshlands. A detailed analysis has been carried out to reduce losses and to specify efficiencies of individual components. As a result of the analysis using the model, it can be seen that, salt rejection can be reduced from 97% to 88% to obtain high quantities of fresh water with an agriculturally acceptable (lower quality). Increasing water feed temperature or reducing the feed water pressure, and physically by increasing the average pore size diameter, led to significantly reduced power energy consumption. Moreover, the specific energy was reduced from 2.8 kWh/m^3 to a more economical 0.8 kWh/m^3 by producing high quantities of drinking water. In addition, it was demonstrated that utilizing energy recovery device turbine and PX in brackish feed water led to a further power saving of around 30% and over 50% respectively. Another interesting finding was that total water cost of a MOD brackish water plant with a total capacity of 24,000 m^3/d and feed salinity of 15,000 ppm (obtained product <400 ppm) is GBP £0.11 /m^3 and the investment costs is GBP £14.4 million, and the cost of production for irrigation) 24,000 m^3/d, feed salinity of 15,000 ppm and obtained product <1600 ppm) is GBP £0.9 /m^3 and with an investment cost of GBP £11.3 million.

Acknowledgments

This work is carried out in line with the research projects funded by the Research Council UK (RCUK) Energy Programme entitled PRO-TEM Network: Process Industry Thermal Energy Management Network (Project No. EP/G059284/1) and Thermal Management of Industrial Processes (Project No. EP/G056706/1). The authors would like to thank the RCUK for providing the funding to sustain the network which has significantly helped to promote the interest in sustainable solutions in order to create a low carbon future and a highly efficient use of energy in the process industries. We would also like to thank Mr N.M. Eshoul in his support in developing and validating the numerical model. Data supporting this publication is openly available under an 'Open Data Commons Open Database License'. Additional metadata are available at: http://dx.doi.org/10.17634/123881-2. Please contact Newcastle Research Data Service at rdm@ncl.ac.uk for access instructions.

References

[1] S. Mitra, et al., Simulation study of a two-stage adsorber system, Appl. Therm. Eng. (2014).
[2] B. Peñate, L. García-Rodríguez, Current trends and future prospects in the design of seawater reverse osmosis desalination technology, Desalination 284 (2012) 1–8.
[3] D.E. Sachit, J.N. Veenstra, Analysis of reverse osmosis membrane performance during desalination of simulated brackish surface waters, J. Membr. Sci. 453 (2014) 136–154.
[4] P.-K. Park, et al., Full-scale simulation of seawater reverse osmosis desalination processes for boron removal: effect of membrane fouling, Water Res. 46 (12) (2012) 3796–3804.
[5] X. Zheng, et al., Seawater desalination in China: retrospect and prospect, Chem. Eng. J. 242 (2014) 404–413.
[6] S. Lattemann, T. Höpner, Environmental impact and impact assessment of seawater desalination, Desalination 220 (1–3) (2008) 1–15.
[7] N. Ghaffour, T.M. Missimer, G.L. Amy, Technical review and evaluation of the economics of water desalination: current and future challenges for better water supply sustainability, Desalination 309 (2013) 197–207.
[8] M.A. Darwish, N.M. Al-Najem, Energy consumption and costs of different desalting systems, Desalination 64 (1987) 83–96.

[9] K. Zotalis, et al., Desalination technologies: hellenic experience, Water 6 (5) (2014) 1134.
[10] S. Lee, R.M. Lueptow, Reverse osmosis filtration for space mission wastewater: membrane properties and operating conditions, J. Membr. Sci. 182 (1–2) (2001) 77–90.
[11] C.H. Ahn, et al., Carbon nanotube-based membranes: fabrication and application to desalination, J. Ind. Eng. Chem. 18 (5) (2012) 1551–1559.
[12] M. Kostoglou, A.J. Karabelas, Modeling scale formation in flat-sheet membrane modules during water desalination, AICHE J. 59 (8) (2013) 2917–2927.
[13] Y.-Y. Lu, et al., Optimum design of reverse osmosis seawater desalination system considering membrane cleaning and replacing, J. Membr. Sci. 282 (1–2) (2006) 7–13.
[14] K.P. Lee, T.C. Arnot, D. Mattia, A review of reverse osmosis membrane materials for desalination—development to date and future potential, J. Membr. Sci. 370 (1–2) (2011) 1–22.
[15] M. Wilf, K. Klinko, Performance of commercial seawater membranes, Desalination 96 (1–3) (1994) 465–478.
[16] M. Wilf, K. Klinko, Effective new pretreatment for seawater reverse osmosis systems, Desalination 117 (1–3) (1998) 323–331.
[17] M. Wilf, K. Klinko, Optimization of seawater RO systems design, Desalination 138 (1–3) (2001) 299–306.
[18] A. Siddiqui, et al., Development and characterization of 3D-printed feed spacers for spiral wound membrane systems, Water Res. 91 (2016) 55–67.
[19] H.-G. Park, et al., Effect of feed spacer thickness on the fouling behavior in reverse osmosis process — a pilot scale study, Desalination 379 (2016) 155–163.
[20] B. Jia, et al., Effect of closed-loop controlled resonance based mechanism to start free piston engine generator: simulation and test results, Appl. Energy 164 (2016) 532–539.
[21] W. Zhou, L. Song, T.K. Guan, A numerical study on concentration polarization and system performance of spiral wound RO membrane modules, J. Membr. Sci. 271 (1–2) (2006) 38–46.
[22] U. Caldera, D. Bogdanov, C. Breyer, Local cost of seawater RO desalination based on solar PV and wind energy: a global estimate, Desalination 385 (2016) 207–216.
[23] W. McGivney, S. Kawamura, Cost Estimating Manual for Water Treatment Facilities, John Wiley & Sons, 2008.
[24] R. Huehmer, et al., Cost Modeling of Desalination Systems, 2011.
[25] F. Hernandez-Sancho, M. Molinos-Senante, R. Sala-Garrido, Cost modelling for wastewater treatment processes, Desalination 268 (1–3) (2011) 1–5.
[26] R.S. El-Emam, I. Dincer, Thermodynamic and thermoeconomic analyses of seawater reverse osmosis desalination plant with energy recovery, Energy 64 (2014) 154–163.
[27] UN-ESCWA and BGR, U.N.E.a.S.C.f.W.A., Euphrates River Basin, 2013.
[28] C.J. Richardson, et al., The restoration potential of the Mesopotamian marshes of Iraq, Science 307 (5713) (2005) 1307–1311.
[29] UNEP, Desk study on the environment in Iraq. United Nations Environment Programme, 2003 Available from: http://www.unep.org/pdf/iraq_ds_lowres.pdf.
[30] USAID, Strategies for Assisting the Marsh Dwellers and Restoring the Marshlands in Southern Iraq, 2003.
[31] E. Nicholson, E.P. Clark, The Iraqi Marshlands: A Human and Environmental Study, 2002.
[32] Marshes Research Centre, 2014 Available from: http://en.mowr.gov.iq.
[33] N.K. Kadhim, Feasibility study of AL-Masab AL-Aam water drainage in ThiQar and treatment for irrigation, J. Water Resour. Ocean Sci. 2 (5) (2013) 84.
[34] B.A. Qureshi, S.M. Zubair, Energy-exergy analysis of seawater reverse osmosis plants, Desalination 385 (2016) 138–147.
[35] A. Al-Zahrani, et al., Thermodynamic analysis of a reverse osmosis desalination unit with energy recovery system, Procedia Eng. 33 (2012) 404–414.
[36] J.G. Wijmans, R.W. Baker, The solution-diffusion model: a review, J. Membr. Sci. 107 (1–2) (1995) 1–21.
[37] R.B. Bird, W.E. Stewart, E.N. Lightfoot, Transport Phenomena, John Wiley & Sons, Inc., New York, 2002.
[38] S. Lee, R.M. Lueptow, Membrane Rejection of Nitrogen Compounds, 2001.
[39] M. Cheryan, Ultrafiltration and Microfiltration Handbook, CRC Press, 1998.
[40] R. Rautenbach, R. Albrecht, Membrane Processes, John Wiley and Sons Ltd., West Germany, 1981.
[41] S.A. Avlonitis, M. Pappas, K. Moutesidis, A unified model for the detailed investigation of membrane modules and RO plants performance, Desalination 203 (1–3) (2007) 218–228.
[42] R.W. Baker, Membrane Technology and Applications, John Wiley & Sons, Ltd., Chichester, 2004.
[43] F. Vince, et al., Multi-objective optimization of RO desalination plants, Desalination 222 (1–3) (2008) 96–118.
[44] DOW, Design a Reverse Osmosis System: Design Equations and Parameters, Technical Manual, 2006.
[45] C. Bartels, et al., The effect of feed ionic strength on salt passage through reverse osmosis membranes, Desalination 184 (1–3) (2005) 185–195.
[46] N. Eshoul, et al., Exergy analysis of a two-pass reverse osmosis (RO) desalination unit with and without an energy recovery turbine (ERT) and pressure exchanger (PX), Energies 8 (7) (2015) 6910.
[47] A. Jawor, E.M.V. Hoek, Effects of feed water temperature on inorganic fouling of brackish water RO membranes, Desalination 235 (1–3) (2009) 44–57.
[48] H.-J. Oh, T.-M. Hwang, S. Lee, A simplified simulation model of RO systems for seawater desalination, Desalination 238 (1–3) (2009) 128–139.
[49] M. Wilf, C. Bartels, Optimization of seawater RO systems design, Desalination 173 (1) (2005) 1–12.
[50] A.L. Ahmad, S. Ismail, S. Bhatia, Ultrafiltration behavior in the treatment of agro-industry effluent: pilot scale studies, Chem. Eng. Sci. 60 (19) (2005) 5385–5394.
[51] T. Mohammadi, M. Kazemi Moghadam, S.S. Madaeni, Hydrodynamic factors affecting flux and fouling during reverse osmosis of seawater, Desalination 151 (3) (2003) 239–245.
[52] J. Jagur-Grodzinski, O. Kedem, Transport coefficients and salt rejection in unchanged hyperfiltration membranes, Desalination 1 (4) (1966) 327–341.
[53] M. Wilf, et al., The Guidebook to Membrane Desalination Technology, Balaban Desalination Publications, 2007.
[54] H.M. Ettouney, et al., Evaluating the economics of desalination, Chem. Eng. Prog. 98 (12) (2002) 32–40.
[55] I. Moch, J. Moch, A 21st Century Study of Global Seawater Reverse Osmosis Operating and Capital Costs, in: BHRO1–16, AWWM Conference, March 2003 (Atlanta GA, USA).
[56] N.M. Wade, Proceedings of Desal '92 Arabian gulf regional water desalination SymposiumTechnical and economic evaluation of distillation and reverse osmosis desalination processes, Desalination 93 (1) (1993) 343–363.
[57] A. Malek, M.N.A. Hawlader, J.C. Ho, Design and economics of RO seawater desalination, Desalination 105 (3) (1996) 245–261.
[58] M.G. Marcovecchio, P.A. Aguirre, N.J. Scenna, Global optimal design of reverse osmosis networks for seawater desalination: modeling and algorithm, Desalination 184 (1–3) (2005) 259–271.
[59] A.M. Helal, S.A. Al-Malek, E.S. Al-Katheeri, Economic feasibility of alternative designs of a PV-RO desalination unit for remote areas in the United Arab Emirates, Desalination 221 (1–3) (2008) 1–16.
[60] R. Turton, et al., in: T.E. Pearson (Ed.), Analysis, Synthesis and Design of Chemical Processes, 2012.
[61] H.T. El-Dessoudy, H.M. Ettouney, Fundamentals of Salt Water Desalination, 2002.
[62] V. Romero-Ternero, L. García-Rodríguez, C. Gómez-Camacho, Thermoeconomic analysis of a seawater reverse osmosis plant, Desalination 181 (1–3) (2005) 43–59.
[63] N.M. Wade, Distillation plant development and cost update, Desalination 136 (1–3) (2001) 3–12.
[64] A. Bejan, G. Tsatsaronis, M.J. Moran, Thermal Design and Optimization, John Wiley & Sons, 1996.
[65] A.A. Al-Karaghouli, L.L. Kazmerski, Renewable Energy Opportunities in Water Desalination, INTECH Open Access Publisher, 2011.
[66] D. Zarzo, E. Campos, P. Terrero, Spanish experience in desalination for agriculture, Desalin. Water Treat. 51 (1–3) (2012) 53–66.
[67] S. Chaudhry, Unit Cost of Desalination, California Desalination Task Force, California Energy Commission, Sacramento, California, 2003.
[68] M.D. Afonso, J.O. Jaber, M.S. Mohsen, Brackish groundwater treatment by reverse osmosis in Jordan, Desalination 164 (2) (2004) 157–171.
[69] S.A. Avlonitis, Operational water cost and productivity improvements for small-size RO desalination plants, Desalination 142 (3) (2002) 295–304.
[70] I.C. Karagiannis, P.G. Soldatos, Water desalination cost literature: review and assessment, Desalination 223 (1–3) (2008) 448–456.